JKAU: Earth Sci., **vol. 16,** pp: 67-93 (2005 A.D. / 1426 A.H.)

Application of Magnetic and Electrical Geophysical Methods in the Exploration of Groundwater Resources of Wadi Malakan, Saudi Arabia

Mansour Abdullah Al-Garni
Department of Geophysics, Faculty of Earth Sciences,
King Abdulaziz University
P.O. Box 80206, Jeddah 21589, Saudi Arabia
maalgarni@kau.edu.sa

Received: 13/12/2004 Revised: 1/5/2005 Accepted: 24/5/2005

Abstract. Magnetic and DC resistivity methods are utilized at Wadi Malakan, Makkah Al-Mukarramah region, Saudi Arabia. Land magnetic survey is conducted to identify the main structure and the depth to the basement along the surveyed part of the wadi. 2-D Euler deconvolution technique is used and reveals the depth to magnetic sources and possible faults that may affect the groundwater flow. Profiling using Wenner array is used to identify the minimum resistivity value along each profile to provide the optimum location for conducting sounding. Sounding using Schlumberger array is used to delineate the saturation zones and the depth to basement at most significant selected sites. The integration between magnetic and DC resistivity methods provides valuable information about the possible location of saturated zones at the conducted part of the wadi. The results of the interpreted vertical electrical resisitivity soundings at VES6004 and VES6010 are confirmed by drilling. The coefficient of anisotropy is calculated and found to be very low which reveals that there is no preferential direction for current flow in which the average transverse resistivity is almost the same as the average longitudinal resistivity which implies that the wadi deposits are not stratified.

Introduction

Wadi Malakan is bounded by latitudes 21º00'N -21º13'N and longitudes 39º33'E and 40º20'E and is located at a distance of about 15 km south of Makkah city (Fig. 1). It is considered an important resource for water supply to Al-Haram for pilgrims use.

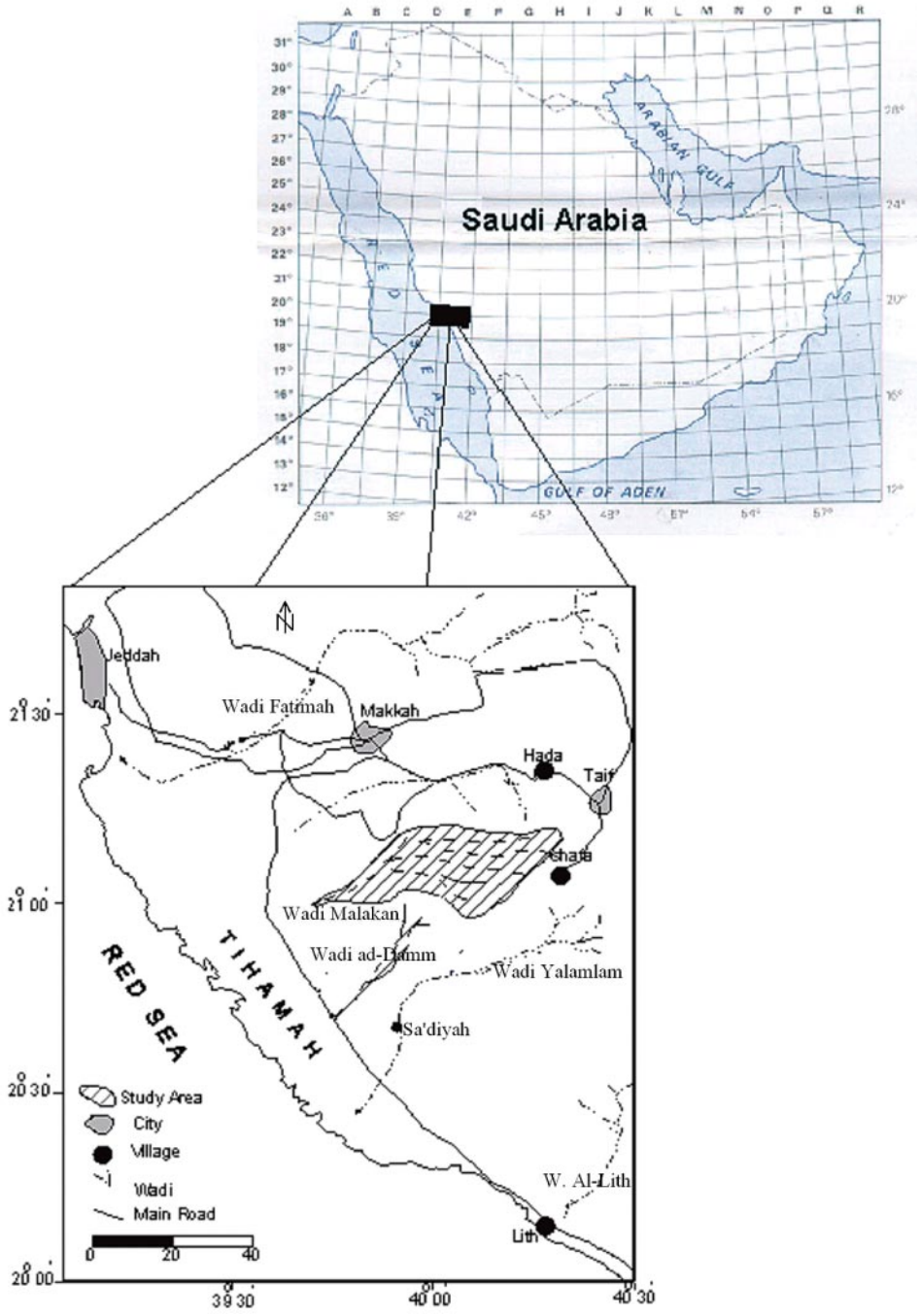

FIG. 1. Location map of the study area.

Wadi Malakan runs through the middle of the Arabian Shield to the Red sea. Specific detailed geological studies were conducted by Moore and Al-Rehaili (1989) as a part of the Makkah Quadrangle and Pallister (1986) as a part of the Al-Lith Quadrangle. Sogreah (1968), German Consult (1979) and Dames and Moore (1988) studied most of the wadis in west and southwest regions of the Arabian Shield and Tihama for water resources and agriculture development. Generally, the potential aquifers of the Arabian Shield are divided into generalized aquifers and discontinuous aquifers (Torrent and Sauveplan, 1977). The generalized aquifers are characterized by a certain continuity of characteristics in space although varying with heterogeneity of the aquifer material and thickness changes of the formation such as wadi alluvium, surface and coastal deposits and basaltic flows. The discontinuous aquifers such as granular crystalline rocks and non-granular volcanic or metamorphic rocks are characterized by little or no original permeability but with secondary permeability acquired either via physico-chemical alteration or via fissuring and fracturing.

Dames and Moore (2001) carried out preliminary hydrogeological and geophysical studies on Wadi Malakan. Recently, some of the drilled wells have been dried out. Thus, studying and promoting the potential groundwater resources using optimized geophysical tools and new interpretation technique is the aim of this study.

Wadi Malakan drains off a part of the Arabian Shield to the Red Sea coastal plane (Tihama). The Arabian Shield consists of Precambrian volcano-sedimentary rocks, which are covered by Tertiary and Quaternary basaltic flows and alluvial sediments, and were subjected to metamorphism and deformation and was intruded by igneous bodies of different ages and compositions (Brown *et al*., 1963; Pallister, 1986; and Moore and Al-Rehaili, 1989) (Fig. 2).

Saydiyah formation is mainly meta-sedimentary rocks in nature, they are interlayered locally with Baish group, which consists of greenschist to amphibolite-facies metamorphic rocks derived mainly from basaltic to rhyolitic volcanic rocks.

Al-Damm dike complex (Tertiary) is named after Wadi Al-Damm (Pallister, 1982c and 1986). This complex consists of an alkali basalt, hawaiite, trachyte, dacite and rhyolite dikes, which are sub-parallel to parallel dikes (with minor sills) and trend mainly in the N-S direction.

Alluvial deposits comprise the largest (Quaternary) unit in Wadi Malakan, which consist of unconsolidated sand, silt and gravel in the wadi stream, and occur also as terrace deposits along the edges of the wadi.

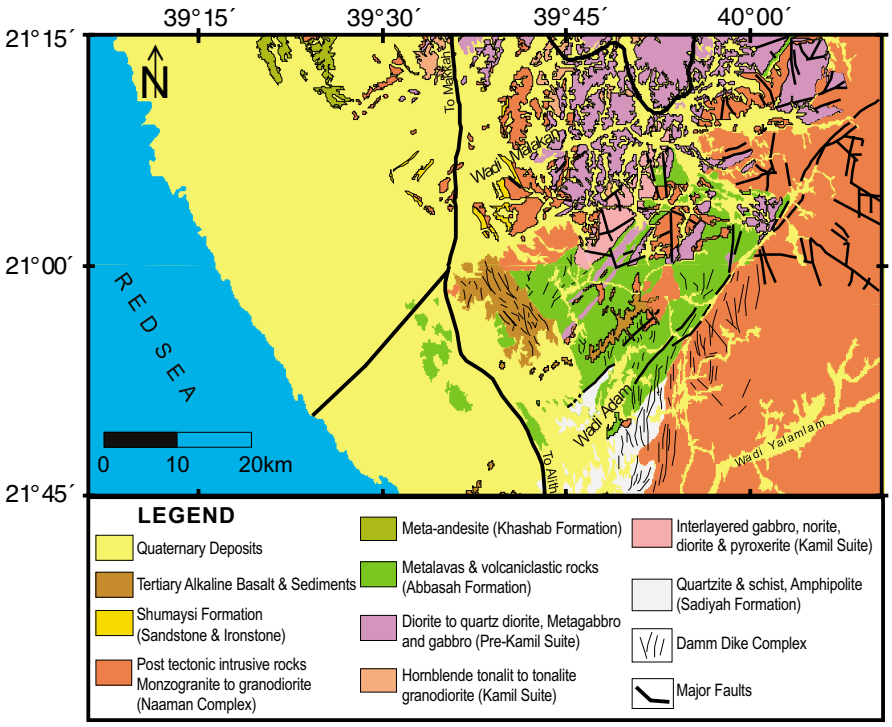

FIG. 2. Geological setting of the study area (Pallister, 1986).

Shumaysi formation is of Tertiary age and unconformably overlies proterozoic rocks of the Baish group and Fatimah formation. It is a sequence of sandstone, siltstone and oolitic ironstone deposited in down faulted basins during Tertiary times and its outcrop is remarkable along the sides of the wadi (Pallister, 1986).

The Arabian Shield has been affected by several orogenic episodes and major younger fault systems of the Oligocene and Miocene age that trend N-W parallel to the Red Sea. Uplifting and faulting led to the development of steep escarpments along the Red Sea coast which is traversed by several deep wadis. These deep wadis are known for frequent flash floods and slow down when crossing the coastal plain until they reach the Red Sea. The gabbroic rocks of Ghumayaqah complex are widely spaced in the form of dikes, which mainly trend in the N-W direction, intruding the metavolcanic rocks.

Twenty three wells are drilled in Wadi Malakan (Fig. 3). Some of these wells are dried out with only few wells are still producing water to Al-Haram. With increasing demand of groundwater for pilgrims uses at Al-Haram, research and exploration were needed to find new well sites in that area. Table 1 shows the well type, well diameter, depth to water, total depth, electrical conductivity, pH,

and daily pumping (Subyani *et al.*, 2004). Magnetic and direct current (DC) resistivity measurements were conducted along profiles. These profiles were chosen based on the request of the people of Malakan water station, sector of ministry of water and electricity, to be accessible for the available electricity line in that wadi. Magnetic data were measured along four profiles, three profiles across the wadi and a profile along the valley, to estimate the depth to the basement and map possible structures that may control the groundwater flow. DC resistivity profiling and sounding were conducted along the three profiles across the wadi to study the resistivity of the overburden sediments with mapping possible saturation zones for new well sites.

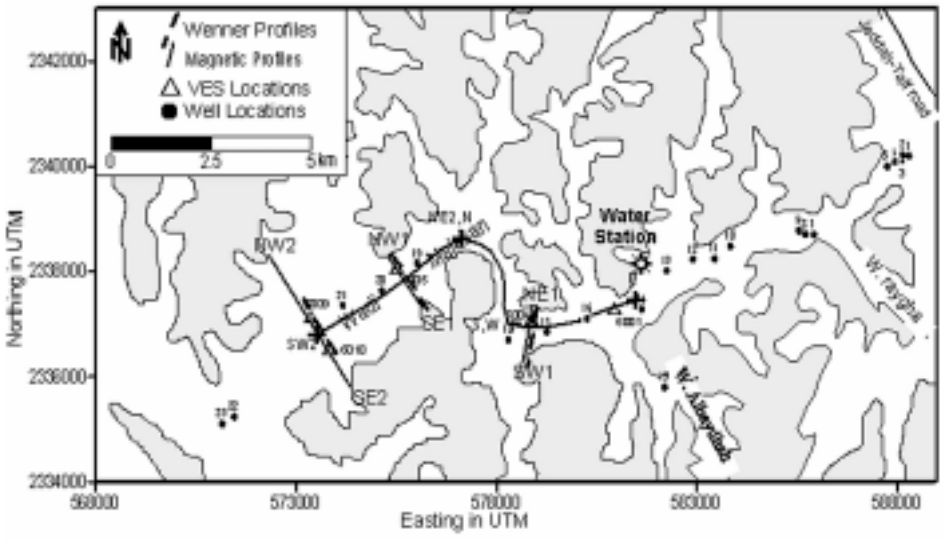

FIG. 3. Location of geophysical surveys.

TABLE 1. Wells of Wadi Malakan, masl = meters above sea level, L = large-diameter well, S = small-diameter drilled borehole, P7 = piezometers with its number, Uk = unknown, Dp = daily pumping, hrs = hours (Subyani *et al.*, 2004).

Well no.	Elevation (masl)	Well type	Diam. (m)	Depth to water (m)	Total depth (c)	E.C. µs/um	pH	Temp. (ºC)	Remark
1	204	L	2.7	26.3	30	2600	7.3	34.7	Dp 7hrs
2	203	L	2.7	27.2	32				Dp, 10hrs
3	201	S	0.3	Uk	41		7.3	31.5	Dp, 10hrs
4	200	L	2.0	27	27.3		7.3	32	Abandoned
5	197.5	S	0.3	Uk	28	3400			Dp, 3 hrs

Table 1. Contd.

Well no.	Elevation (masl)	Well type	Diam. (m)	Depth to water (m)	Total depth (c)	E.C. µs/um	pH	Temp. (ºC)	Remark
6	203	S	0.3	30.1	35.4	2600	7.5	33	Dp, 3 hrs
7	189	S	0.3	Uk	35	3700	7.2	32	Dp, 7hrs
8	188	S		Uk	Uk				
9	186.5	S	0.3	25.85	38	3300	7.4	34.5	Dp, 6hrs
10	181	L	1.9	33.1	42	3660	7.3	35	Dp, 1hr
11	180.5	L	2.5	28.9	43				Dp, 3 hrs
12	179	S	0.3	Uk	Uk	2920	7.3	34	Sealed
13	177	L	?	30	41.5	3350	7.4	35	Dp, 7hrs
14	176	P	0.05	31.6	39				P1
15	195	L	2	45	2.5	3600	7.3	31	Dp, 3 hrs
16	172	P	0.05	Uk	Uk	2000	7.2	31	P2
17	166	L	?	33	3				New
18	160	P	0.05	32.44	45.22				P3
19	153	P	0.05	35.94	47				P4
20	152	P	0.05	40.05	48				P5
21	146	P	0.05	39.1	43	2900	7.3	33	P6
22	136	P	0.05	39.45	42				P7
23	133	P	0.05	36.9	44	2950	7.3	33	P8

Geophysical Survey and Interpretation Techniques

High Resolution Land Magnetic Survey

The magnetic data were collected along four profiles in Wadi Malakan (Fig. 3). Two profiles trend SE-NW, a profile trends SW-NE, and the fourth profile is divided to three profiles and trends SW-NE, N-S and W-E. Three profiles SW1-NE1, SE1-NW1 and SE2-NW2 extend about 1.25, 0.7 and 3 km, respectively. The fourth profile which was surveyed along the wadi extends about 8.6 km. The station interval was chosen differently based on the purpose of the conducting survey. The station interval of the profile along the wadi was chosen to be about 100 m which was designed for the purpose of recognizing the major structures

that may affect the groundwater flow. However, the station interval of the three profiles crossing the wadi was surveyed at about 10 m in order to recognize the possible structures that may exist and affect the groundwater flow and approximating the sedimentary deposits. Thus, the results would be very helpful in verifying the profiling survey using DC resistivity and then conducting a vertical electrical sounding (VES) at the best location along these profiles. By knowing the structures and the depth to basement, the optimum location for the potential of groundwater may be determined. Therefore, magnetic data interpretation along the four profiles provides approximations of the thickness of the sedimentary deposits and the structure across and along the interesting part of the wadi.

The total magnetic intensity component was measured using the proton precession magnetometer (ENVI-Mag, SCENTRIX). A total of 346 readings were recorded along the four profiles in which 119 readings along SW1-NE1 profile, 78 readings along SE1-NW1, 99 readings along SE2-NW2, and 50 readings along the profile that was surveyed along the wadi.

Magnetic Data Processing and Interpretation

Generally, magnetic data are interpreted by estimating source rock depths or locations (Vacquier *et al*., 1951). Spector and Grant (1970) addressed depth estimation utilizing slope of the power spectral density in statistical sense. Cordell and Grauch (1985) calculated the horizontal gradient of the pseudogravity for boundary location, which peaks over a vertical contact; however, the peak is somewhat offset for dipping contacts. Nabighian (1972, 1974 and 1984) found that the total gradient or analytical signal peaks are directly over arbitrary dip contact but is somewhat noisy estimator (Hansen *et al*., 1987). The width of the peak is utilized to estimate the depth to the causative source.

Numerous automatic processing methods join source location and depth estimation (Thompson, 1982). Werner deconvolution method fits elementary models to successive segments of a profile and successfully estimates source location, depth and dip (Hartman *et al.*, 1971; Jain, 1976). Naudy (1971) used a similar approach employing prism and thin plate models. Solving for the causative body positions and obtaining an indication of causative body type were described by Thompson (1982), who provided a method which utilized Euler's equation to successive segments of a pole-reduced profile. Reid *et al.* (1990) described a fast means of processing magnetic data to drive trends and depth estimates in an automatic or semiautomatic algorithm.

The magnetic profiles in the present study are quantitatively interpreted using Euler deconvolution technique because it is both a boundary finder and a depth estimator (Reid *et al*., 1990). Generally, Euler deconvolution has been ex-

tensively used for interpreting the magnetic data such as tracing geological contacts (boundaries) and obtaining estimates of the depth of the causative sources (Reid *et al*., 1990; Stavrev, 1997; Stavrev *et al*., 2003; and many others). It is appropriate to mention here the Euler's homogeneity equation which can be written as (Reid *et al*., 1990).

$$(x - x_0)\, dT / dx + (y - y_0)\, dT / dy + (z - z_0)\, dT / dz = N\,(B - T) \qquad (1)$$

where T the observed magnetic field at (x, y, z),

(x_0, y_0, z_0) the causative source location,

B the base level of the observed field, and

N denotes the source geometry and known as the structural index (SI) (Thompson, 1982).

Euler method applies to functions that are homogeneous, which is usually the case for magnetic field due to contacts, thin dikes and poles (Keating and Pilkinton, 2004). Magnetic data do not need to be reduced to pole and is considered not an interfering factor (Reid *et al*., 1990). Two-dimension (2-D) problems, which is considered in this study, two terms with x and z should be kept while the others are neglected. Therefore, the 2-D Euler's homogeneity equation can be written as:

$$(x - x_0)\, dT / dx + (z - z_0)\, dT / dz = N\,(B - T) \qquad (2)$$

Evaluating T and its two derivatives at all points (x, z) on the observed magnetic data requires obtaining a system of simultaneous equations and then the unknown parameters are the locations of the source(x_0, z_0), N, and the magnetic field, B. However, this method does not provide a solution for N directly, but rather makes a series of calculations of source position (x_0, z_0) for a number of assumed values of N (Reid *et al*., 1990). The right choice value of N would provide correct values position(x_0, z_0) of the causative source. In this paper, N was chosen based on the available geological information as well as the depth that was provided by the vertical electrical sounding (VES6004), where the depth to the basement is about 42 m, and it is approximately determined to be $N = 0.5$. The depth to the source rock from the Euler deconvolution method shows that the depth at sounding VES6004 is about 50 m. The difference in depth between the DC resistivity and magnetic methods is attributed to the fact that the DC resistivity may be affected by the weathered basement more than the magnetic method. Thus, the geoelectric basement is usually considered to be shallower than the magnetic source rock basement that was obtained from the Euler deconvolution method. The other three unknown parameters are then solved by a matrix inversion from an array of nodes along the profiles with a predetermined window. Furthermore,

we have to keep in mind that the Euler deconvolution method is generally preferred to be used for mapping structures rather than estimating the depth of the basement, which is the most interesting part in this study. However, in this study, it provides a reasonable interpretation for the basement depth because of the fact that the *N* is determined based on the interpretation of VES.

The observed upward gradient trending SW-NE (Fig. 4a) and downward gradient trending SW-NE (Fig. 5a and 6a) generally represent the combination effect of the instrumental drift, diurnal variation and the component of the earth's magnetic field along the survey profiles (Al-Garni, 2004). These trends are automatically cancelled during the process of differentiation in the next processing sequence.

Figure 4 (a, b, c and d) show the field data, horizontal and vertical derivatives, Euler deconvolution solution and the earth model, respectively. The magnetic survey along this profile SW1-NE1 using Euler deconvolution method showed that the middle and the northeastern parts have thicker sediments than the southwestern part (Fig. 4c and d). Also, these sediments are clearly associated with a possible fault system along this profile (crossing wadi).

Figure 5 (c and d) shows that the middle and northwestern parts of the profile have thicker sediments than the southeastern part. Therefore, the thickness of the sediments is also clearly related to the proposed system of faults crossing the wadi.

Figure 6 (c and d) shows that this part of wadi has shallow magnetic sources; however, there is an evidence that the northwestern part of the wadi may have thicker sediments than elsewhere and that is clearly because of the associated faults (Fig. 6c and d).

The total magnetic intensity field (Fig. 7a) and the residual magnetic field (7b) along SW2-NE2 and W-E profiles of Wadi Malakan may show that the magnetic anomaly along this profile can be generally divided into three segments A, B, and C (Fig. 7). The A segment is characterized by low magnetic amplitude irregularities of about 35 gammas, the segment B is characterized by well-defined magnetic anomaly of about 130 gammas and the segment C is characterized by a lower magnetic amplitude irregularities of about 50 gammas. However, segment A shows a higher frequency than segment C and that may indicate that the basement at segment A is shallower than at segment C. This was confirmed using Euler deconvolution method on both profiles (Fig. 8 and 9). The different characterizations of the two segments show that there is possibly a major fault as shown in Fig. 7b. Figure 8 shows that the profile that was surveyed along the wadi (SW2-NE2 profile) may have been extensively affected by fault systems and this system caused the high irregularities in the surface of the magnetic source. However, Fig. 9 shows the eastern part of the wadi (W-E

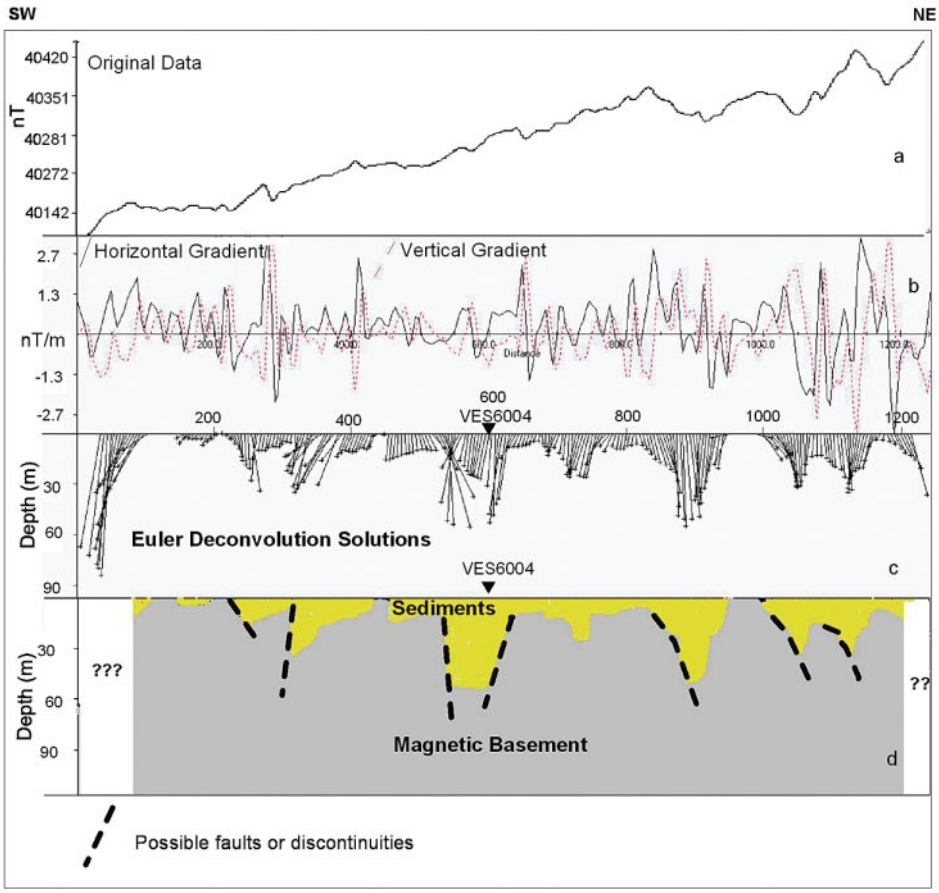

FIG. 4. Euler deconvolution solution for ground magnetic profile SW1-NE1, Wadi Malakan, Makkah, Saudi Arabia. a) Observed field, b) The horizontal (solid line) and vertical gradient (dashed line) fields, c) The Euler deconvolution solution depths, and d) A possible earth model as composed from Euler depths and geologic information available.

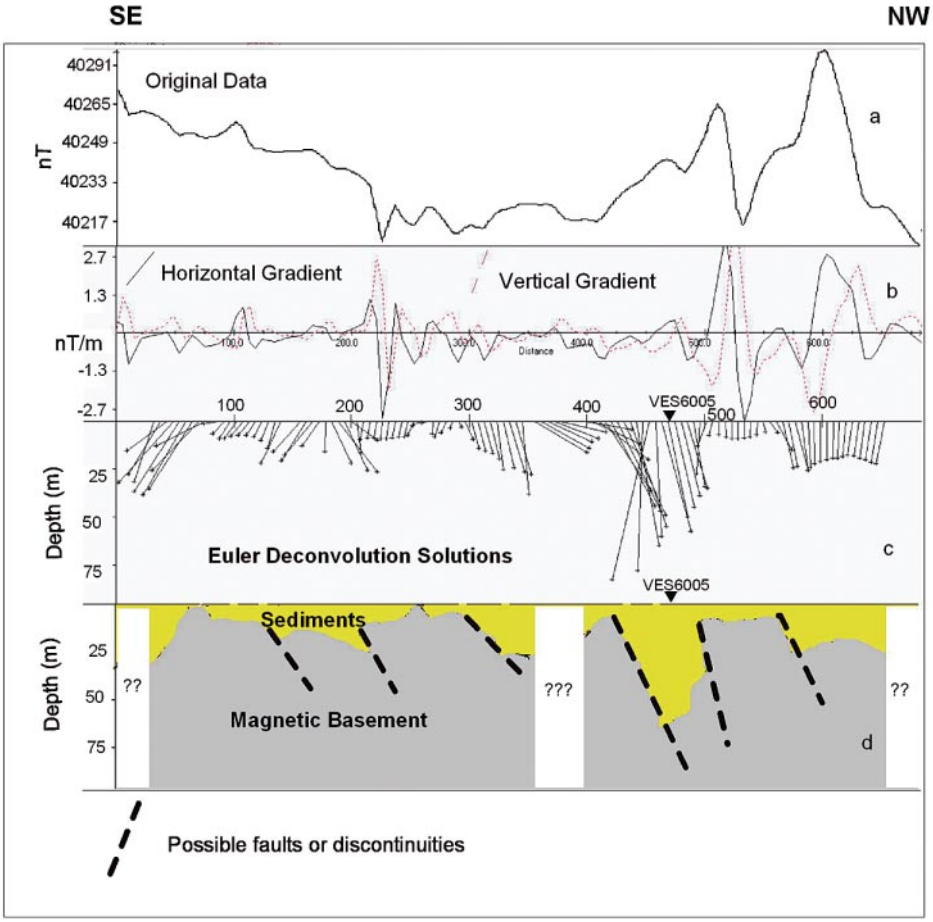

FIG. 5. Euler deconvolution solution for ground magnetic profile SE1-NW1, Wadi Malakan, Makkah, Saudi Arabia. a) Observed field, b) The horizontal (solid line) and vertical gradient (dashed line) fields, c) The Euler deconvolution solution depths, and d) A possible earth model as composed from Euler depths and geologic information available.

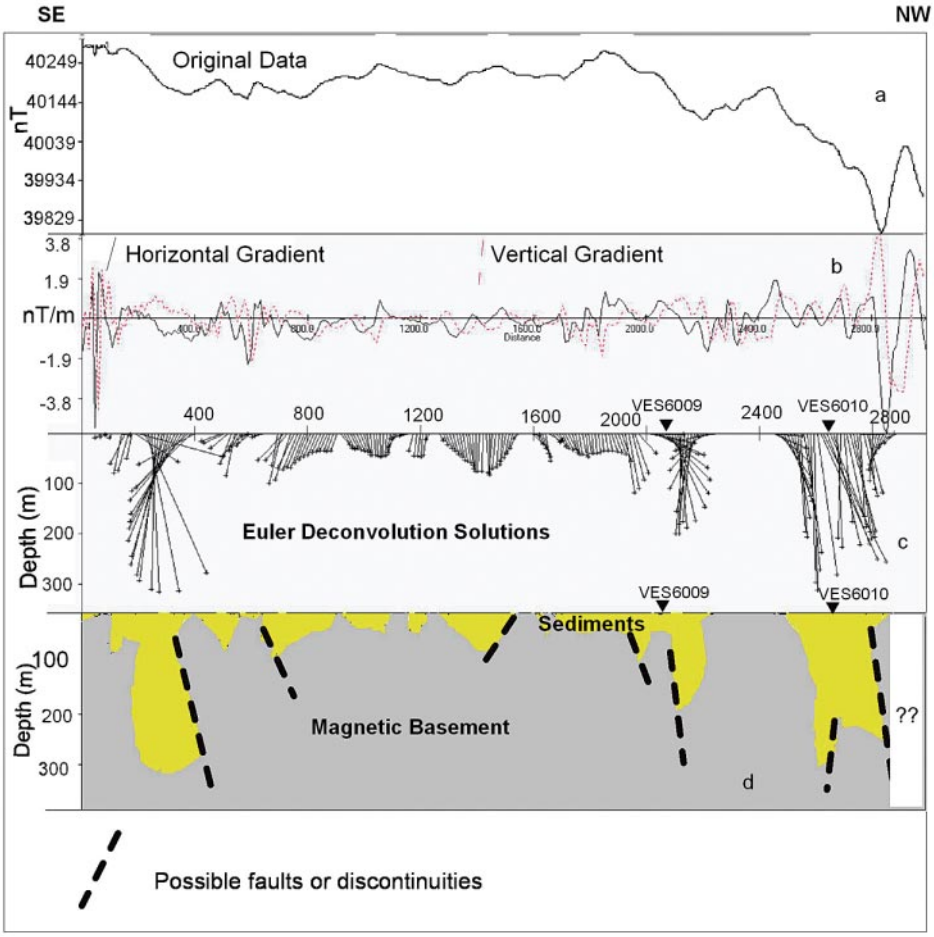

FIG. 6. Euler deconvolution solution for ground magnetic profile SE2-NW2, Wadi Malakan, Makkah, Saudi Arabia. a) Observed field, b) The horizontal (solid line) and vertical gradient (dashed line) fields, c) The Euler deconvolution solution depths, and d) A possible earth model as composed from Euler depths and geologic information available.

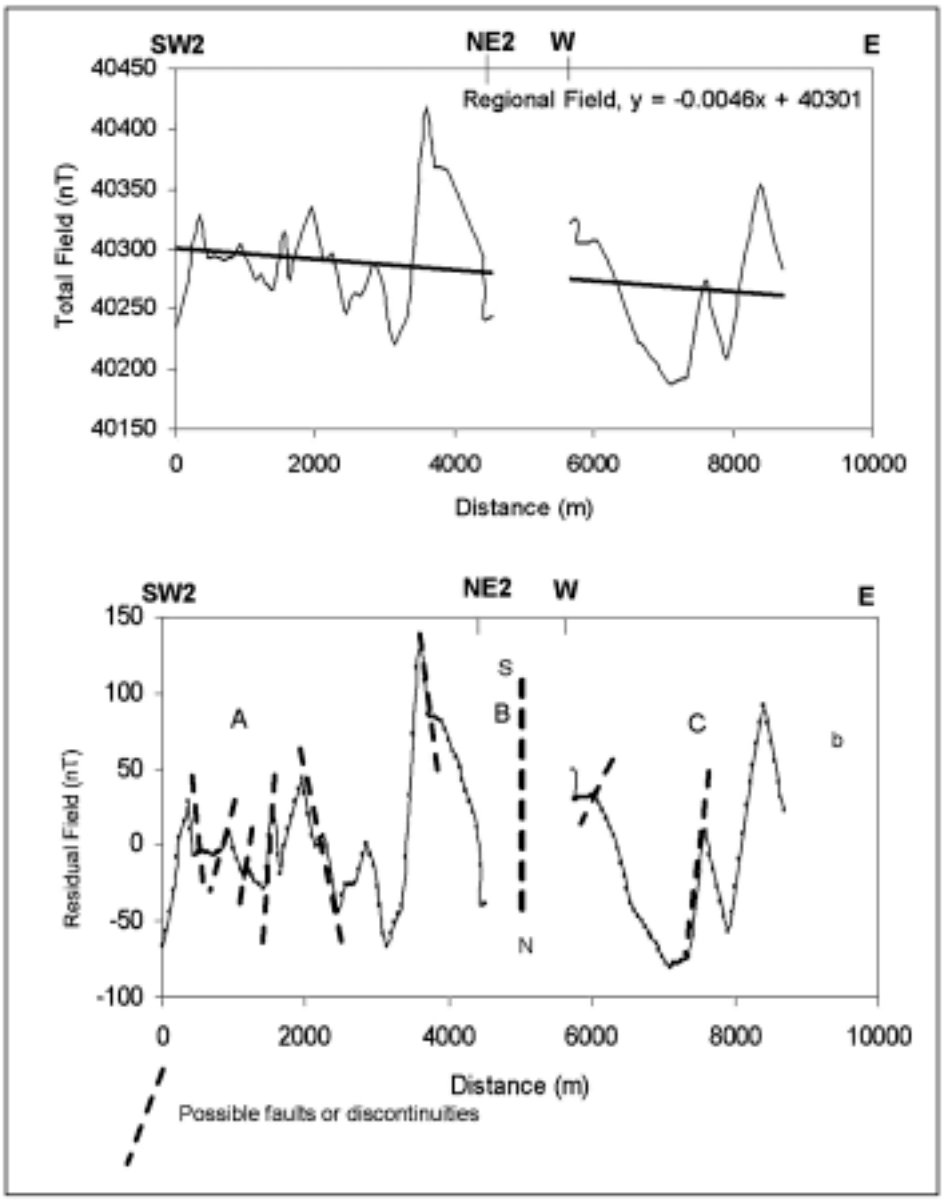

FIG. 7. Magnetic field intensity, a) total field and b) residual field of the removing linear regional component.

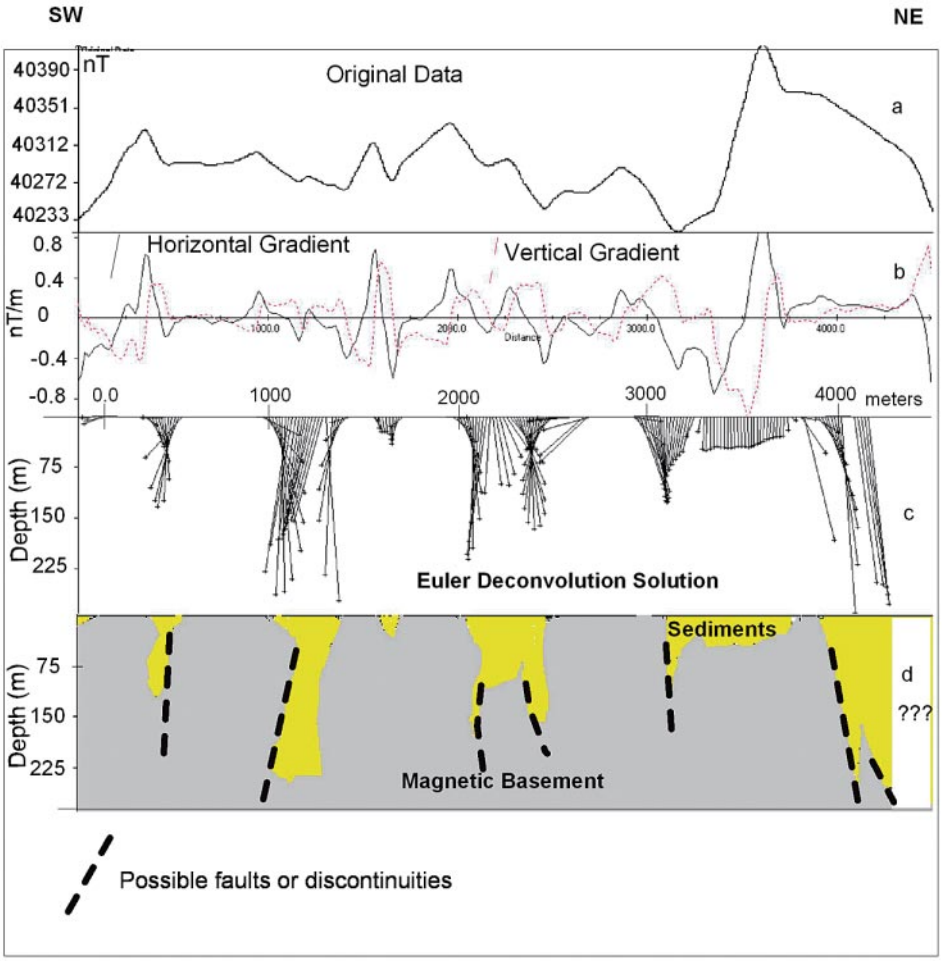

FIG. 8. Euler deconvolution solution for ground magnetic profile SW2-NE2, Wadi Malakan, Makkah, Saudi Arabia. a) Observed field, b) The horizontal (solid line) and vertical gradient (dashed line) fields, c) The Euler deconvolution solution depths, and d) A possible earth model as composed from Euler depths and geologic information available.

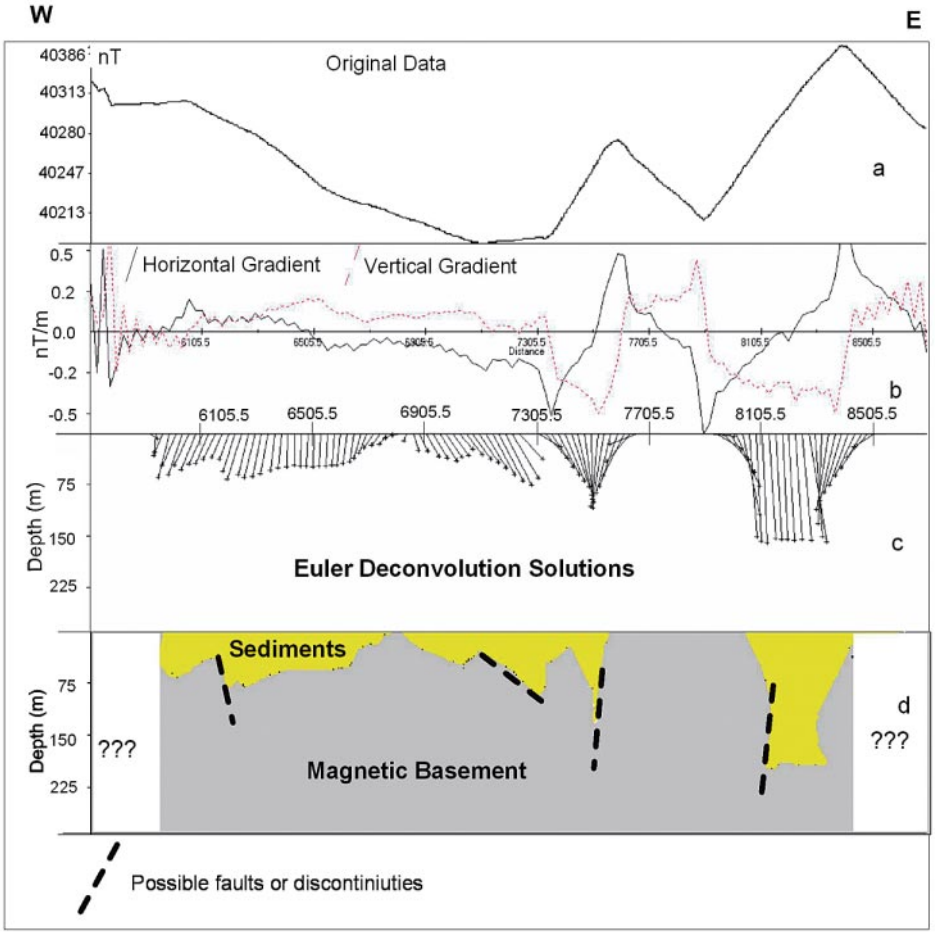

FIG. 9. Euler deconvolution solution for ground magnetic profile W-E, Wadi Malakan, Makkah, Saudi Arabia. a) Observed field, b) The horizontal (solid line) and vertical gradient (dashed line) fields, c) The Euler deconvolution solution depths, and d) A possible earth model as composed from Euler depths and geologic information available.

profile) possibly have been affected by lesser faults which make this part more gentle than the other side. Figure 10 shows the Euler deconvolution solution along the total magnetic intensity curve of profile (N-S) and declare two possible faults along this profile in the south part of the profile.

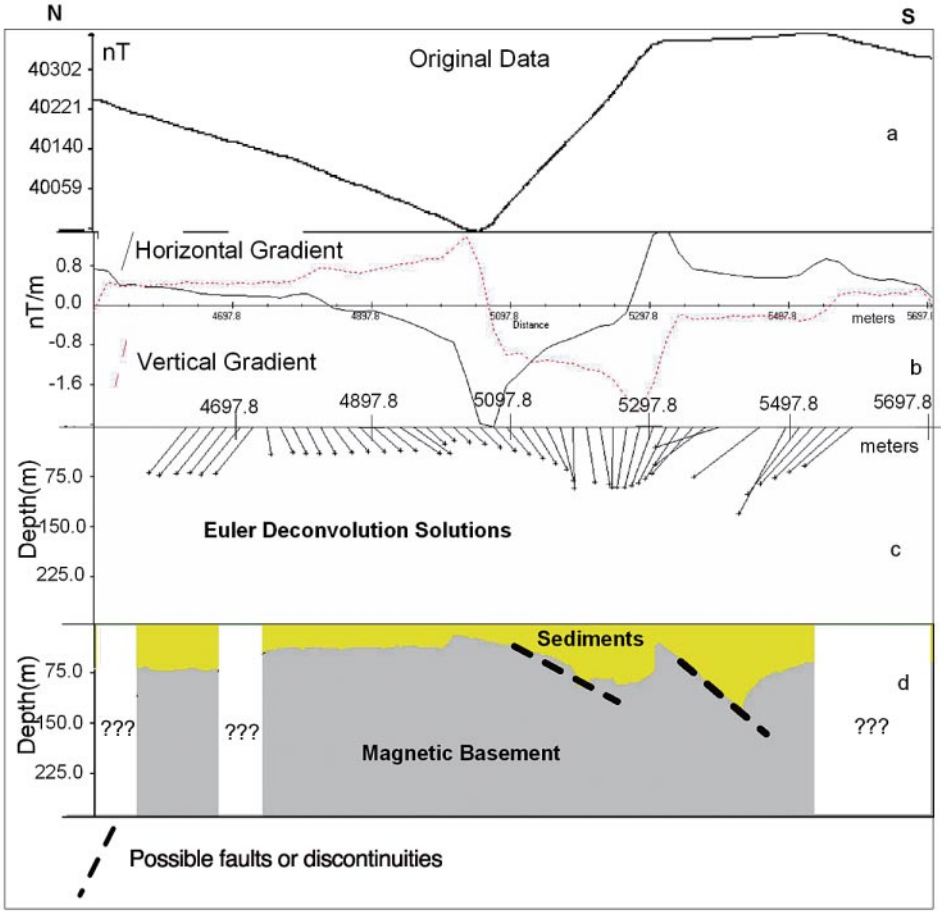

FIG. 10. Euler deconvolution solution for ground magnetic profile N-S, Wadi Malakan, Makkah, Saudi Arabia. a) Observed field, b) The horizontal (solid line) and vertical gradient (dashed line) fields, c) The Euler deconvolution solution depths, and d) A possible earth model as composed from Euler depths and geologic information available.

Electrical Survey

The vertical electrical sounding (VES), studying the vertical variation of resistivity, and profiling, studying the lateral variation of resistivity, were conducted along three profiles across Wadi Malakan where that magnetic method is conducted. Profiling survey was conducted along each profile using Wenner array and the sounding was conducted using Schlumberger array. Profiling survey was conducted along each profile SW1-NE1, SE1-NW1 and SE2-NW2 with electrode spacing a = 50 m except profile SW1-NE1 which was also surveyed with a = 20 (Fig. 11-13). Then, the sounding survey was conducted at locations where the minimum resistivity is pronounced. Figure 14 shows a total of 5 Schlumberger sounding field curves that have been made at selected sites on Wadi Malakan (Fig. 3). Figure 19 shows the VES at a location near well 14 which was conducted in order to have a possible water supply close to the station. The maximum current electrode spacings (AB/2) ranged from 140 to 200 m. The geophysical electrical sounding data were collected using 1200 watts DC resistivity meter, ELREC-T pulse, IRIS made.

Apparent resistivity would be measured because the ground is not composed of homogeneous isotropic half space and then would depend on the geometry, the spacing, and the orientation of the electrode array with respect to lateral inhomogeneities and the spatial distribution of materials with different electrical resistivities (Zohdy *et al.*, 1994; Al-Garni, 1996).

Electrical Sounding Processing and Interpretation

The sounding curves were interpreted using an automatic interpretation computer program (Zohdy, 1989). This program uses an iterative scheme which does not require an initial guess of the number of layers, their thicknesses, or their resistivities. Extrapolating incomplete sounding curves are not required as well. Its layering model is shown as step function which represents the variation of resistivity beneath the middle of the electrode array with depth. Sounding curves are interpreted based on the assumption of horizontally stratified layers.

Electrical resistivity gives an excellent indication to distinguish between the saturated zones from the unsaturated zones. Many other parameters such as lithology, grain size, clay content, salinity, and depth affect the electrical resistivity. Five vertical electrical resistivity soundings were constructed (Fig. 15-19). The interpreted vertical electrical soundings are derived from the step function resistivity layers (Zohdy, 1989).

Figure 15 shows the interpretation of VES6004. It shows that the water-bearing zone is located at depth of about 20 m and extending to about 42 m. The zone extending from the surface to at depth of about 20 m has a resitivity >

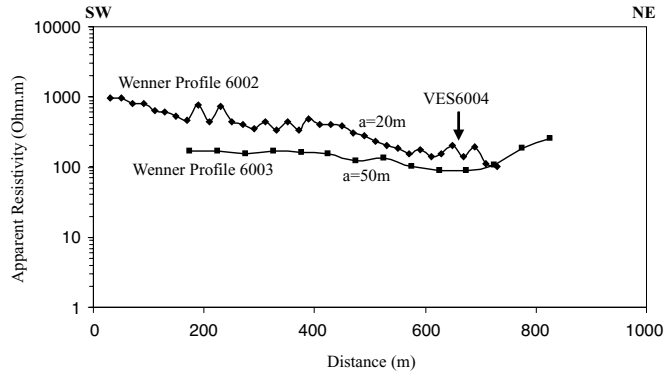

FIG. 11. Wenner profiling along profile SW1-NE1 showing the minimum value of resistivity and the location of VES6004.

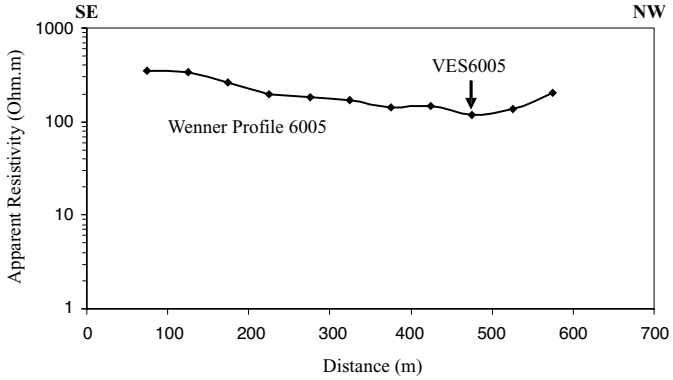

FIG. 12. Wenner profiling along profile SE1-NW1 showing the minimum value of resistivity and the location of VES6005.

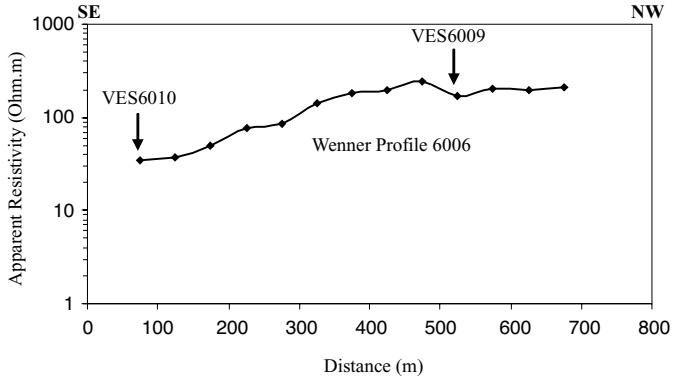

FIG. 13. Wenner profiling along profile SE2-NW2 showing the minimum value of resistivity and the locations of VES6010 and VES9009.

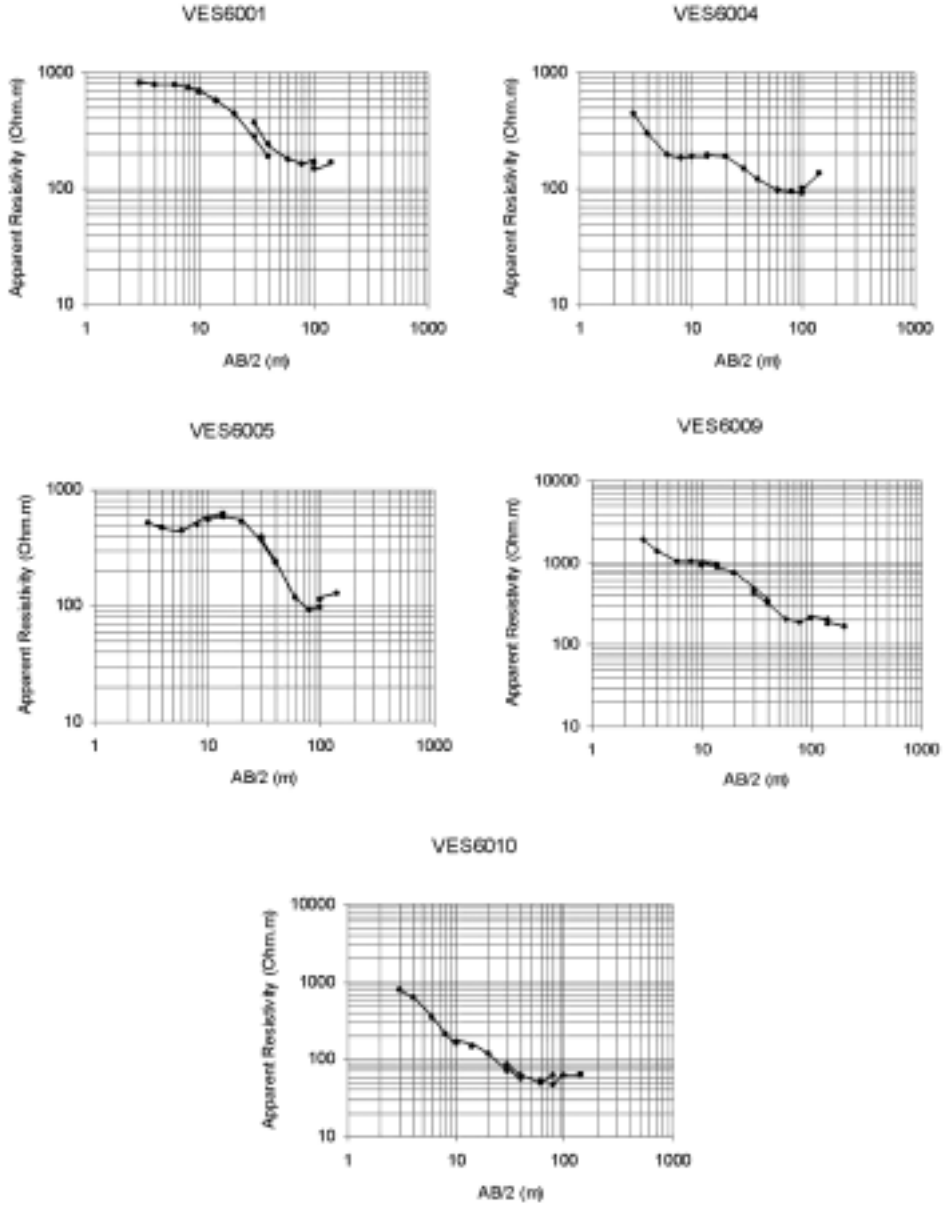

FIG. 14. Field curves of the vertical electrical sounding VES6001, VES6004, VES6005, VES6009 and VES6010.

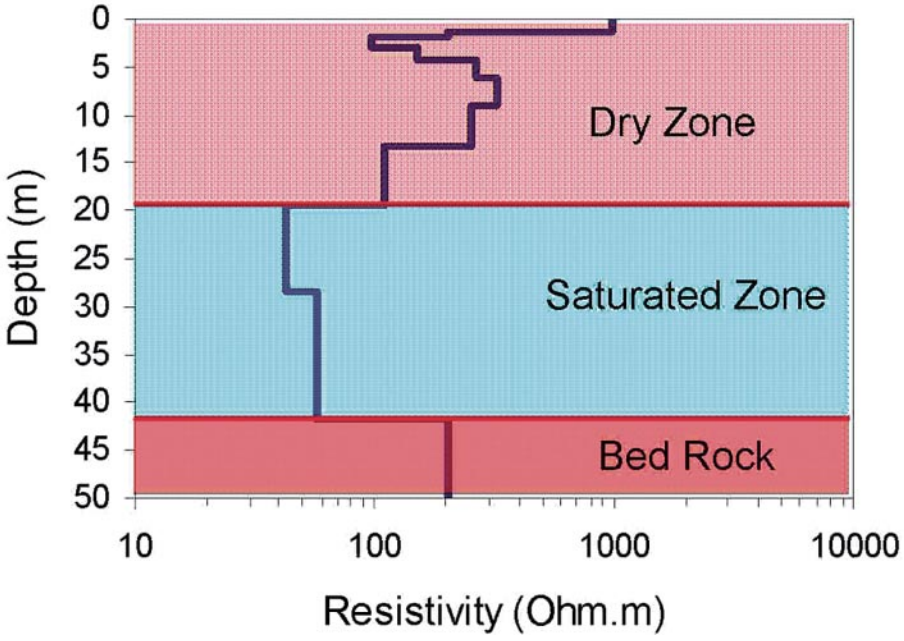

FIG. 15. Interpreted geoelectrical resistivity depths model beneath VES6004.

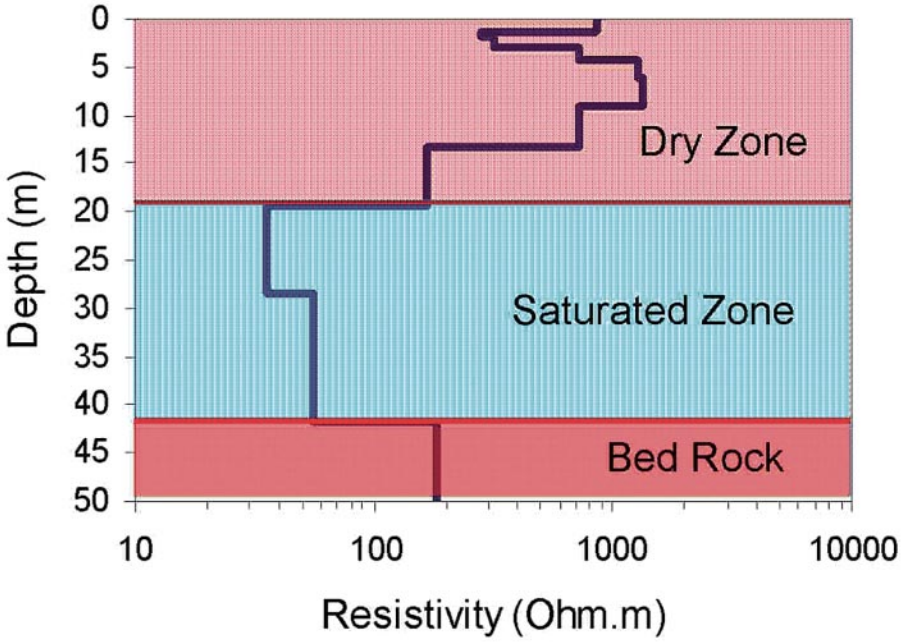

FIG. 16. Interpreted geoelectrical resistivity depths model beneath VES6005.

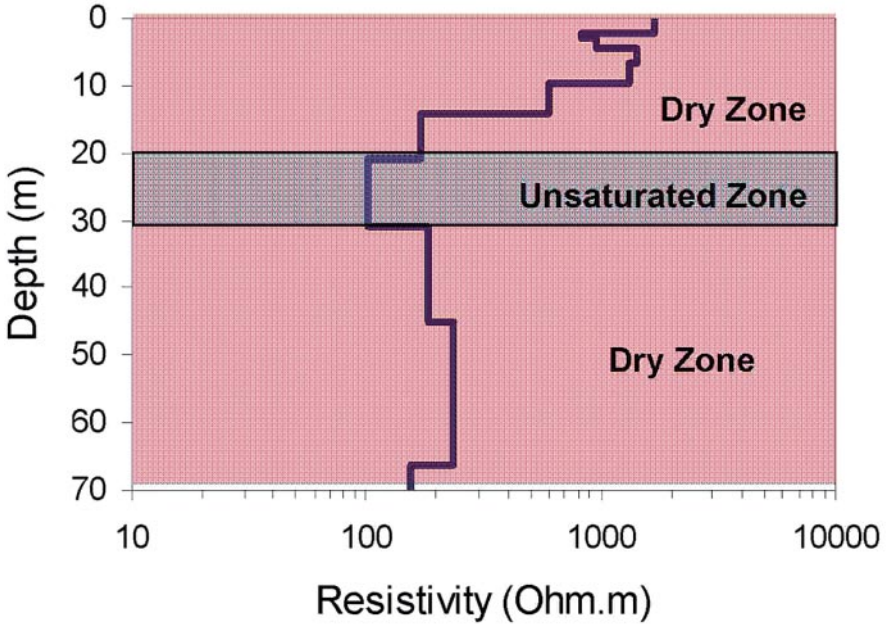

FIG. 17. Interpreted geoelectrical resistivity depths model beneath VES6009.

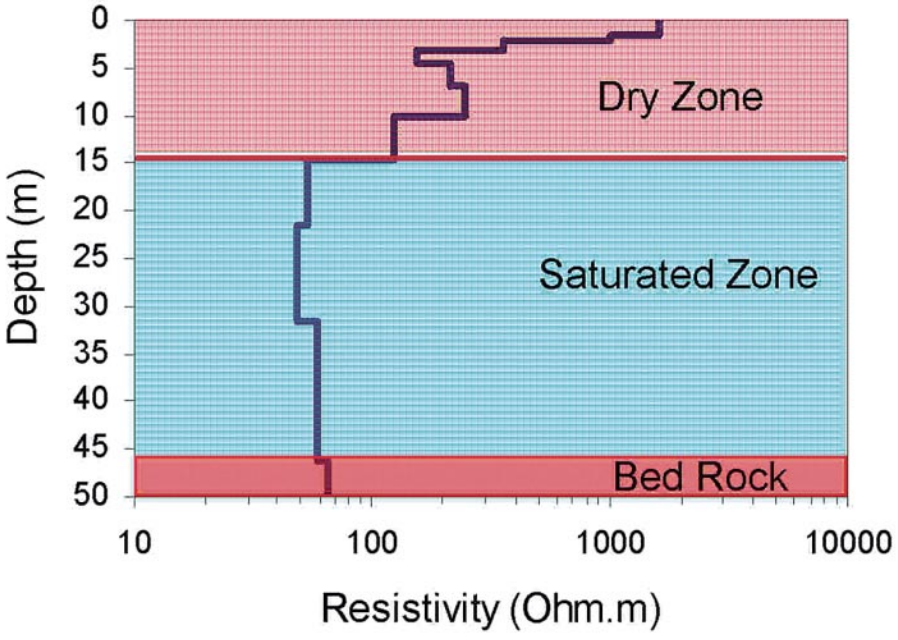

FIG. 18. Interpreted geoelectrical resistivity depths model beneath VES6010.

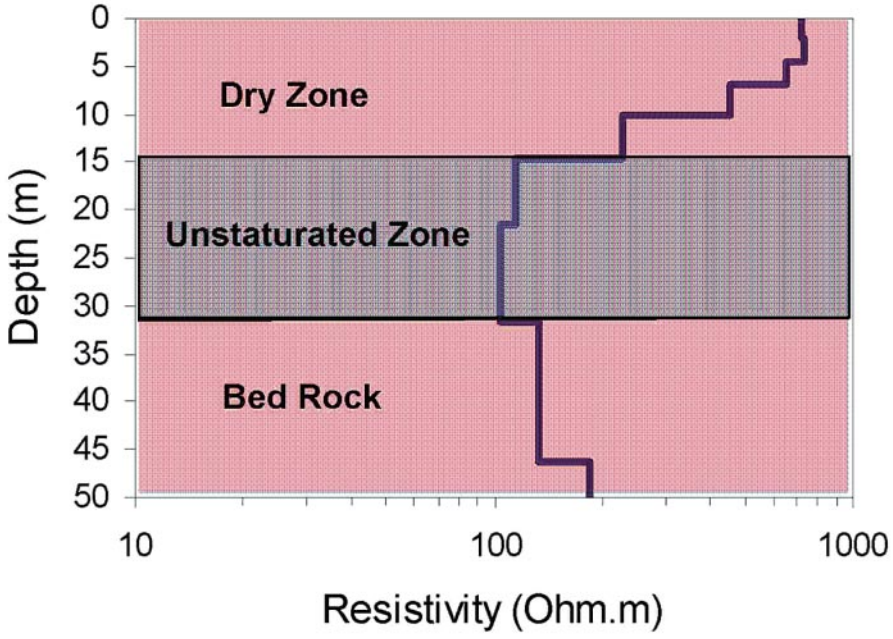

FIG. 19. Interpreted geoelectrical resistivity depths model beneath VES6001.

100 Ohm.m may represent unsaturated near surface sand, gravel and cobbles. The zone extending from about 20 m to about 28 m has a resistivity of about 42 Ohm.m may represent sedimentary deposits of fine sand with low percentage of clay saturated with good quality water. The zone extending from about 28 m to about 40 m has a resistivity of about 55 Ohm.m may represent sedimentary deposits of fine sand, coarse sand, and low percentage of gravel mixed with clay. The high resistivity beneath 42 m represents the geoelectric basement. A drilled exploratory well at the location of VES6004 shows that the main characteristics of the different units are as follows: a) dry zone of sand and gravel extending from the surface to about 18.5 m, b) wet zone of fine sand with low percentage of clay extending from about 18.5 m to about 28 m, c) saturated zone of coarse sand, fine sand and low percentage of gravel with low percentage of clay extending from 28 m to 39.6 m, and d) the geoelectric basement at depth 39.6 m. In DC resistivity method, depths are generally overestimated by a factor equal to the anisotropy coefficient $\lambda = \sqrt{\rho_t / \rho_l}$, where ρ_t and ρ_l are the transverse and longitudinal resistivities, respectively (Zohdy *et al.*, 1974 and Al-Garni, 1996). The values of λ generally range > 1 to 1.3 and rarely exceed 2 (Zohdy *et al.*, 1974). The anisotropy coefficient can be calculated by the known true depth (h_{true}) and the interpreted depth ($h_{interp.}$) as follows (Zohdy *et al.*, 1974 and Al-Garni, 1996).

$$\lambda = \frac{h_{interp.}}{h_{true}} \quad (3)$$

Thus, the interpreted resistivity shows an excellent correlation with the true depths and the anisotropy coefficient is approximated to be 1.06.

Figure 16 (VES6005) shows the same interpretation as the previous sounding (VES6004). This location has not been drilled yet; however, same results as the previous sounding (VES6004) are expected.

Figures 17 and 19 show the interpretation of VES6009 and VES6001, respectively. Figure 17 shows an unsaturated zone extending from about 20 m to 30 m and no water-bearing zone found at this location. Figure 19 shows also an unsaturated zone extending from about 15 m to 31 m and no water-bearing zone found at this location. The interpreted resistivity of about 100 Ohm.m may represent unsaturated alluvial deposits of sand, gravel and cobbles. The interpreted resistivity > 150 Ohm.m may indicate dry sedimentary deposits or indicate the basement is being reached (Al-Garni, 1996).

Figure 18 shows the interpretation of VES6010. It shows that the water-bearing zone is located at depth of about 15 m and extending to about 47 m and then the resistivity starts to increase and this is an indication of reaching the basement. The zone extending from the surface to a depth of about 15 m has a resitivity > 100 Ohm.m may represent unsaturated near surface sand, gravel and cobbles. At this location, measurements could not be carried out further because the potential difference reached to less than 3 mV and that would generate noise and unreasonable results. A drilled exploratory well at the location of VES6010 shows that the main characteristics of the different units are as follows: a) dry zone of sand and gravel extending from the surface to about 16 m, b) wet zone of fine sand with some percentage of clay extending from about 16 m to about 35 m, c) saturated zone of coarse sand, fine sand and low percentage of gravel from about 35 to about 46 m, and d) the basement at depth 39.6 m. The anisotropy coefficient (λ) is found to be 1.02.

The calculated coefficients of anisotropy (λ) are small and indicate that the transverse resistivity is almost the same as the longitudinal resistivity. In other words, the wadi is characterized by mixed deposits and not well defined layers.

Discussion and Conclusion

Magnetic and DC resistivity methods are conducted to find new water supply that would be used to supply Al-Haram. These methods provide information about the subsurface geology, saturated zones in the conducted part of Wadi

Malakan. A total of four magnetic profiles were conducted at Wadi Malakan. Euler deconvolution technique has quantitatively delineated the regional structure which controls the groundwater distribution along the conducted part of the wadi. The total magnetic intensity data along the wadi reveals that the area is affected by a N-S fault which may control the underground water flow. Furthermore, it shows that the eastern side of the wadi has thicker sediments than the western part. The high irregularities observed in the western part could be considered as associated and related to the fault zone, contrary to the eastern part which shows rather low irregularities.

Electrical profiling, studying the resistivity variation laterally, using Wenner array survey is conducted along the proposed locations to be near the electricity line. This survey shows the minimum resistivity value along each profile which indicates the sites of subsurface water accumulation. Then, electrical sounding survey using Schlumberger array is conducted at locations where the resistivity is minimum to study the resistivity variation with depth and to delineate the possible saturated zones.

Drilling was implemented at locations VES6004 and VES6010 and reveals an excellent agreement with the interpreted resitivity data. The coefficient of anisotropy was calculated and found to be low which may indicate that the depositional environment at Wadi Malakan and may be other wadis are not of stratified nature and may be explained as made of mixed sediments.

Combination between electrical resistivity profiling and sounding and using magnetic method suggest the possible occurrence of groundwater and the subsurface structures.

Acknowledgment

This work was funded by the Scientific Research Council of King Abdulaziz University, Jeddah, Saudi Arabia. I also would like to thank my colleagues Dr. Hamdy Hassanein and Dr. Mohamed Gobashy for their helpful comments and valuable criticisms.

References

Al-Garni, M.A. (1996) *Direct Current Resistivity Investigation of Groundwater in the Lower Mesilla Valley, New Mexico and Texas*, M.Sc. Thesis, Colorado School of Mines.

Al-Garni, M.A. (2004) Schlumberger sounding and magnetic survey in Wadi Al-Damm, Makkah Al-Mukarramah, Saudi Arabia, *Journal of Petroleum and Mining Engineering*, **7:** 45-60.

Brown, G.F., Jackson, R.O., Bogue, R.G. and **MacLean, W.H.** (1963) *Geology of the Southern Hijaz Quadrangle, Kingdom of Saudi Arabia: DGMR*, Misc., Geologic Inves. Map I-210A, 1:500,000 scale.

Cordell, L. and **Grauch, V.J.S.** (1985) Mapping basement magnetization zones from aeromagnetic data in the San Juan basin, New Mexico, in: Hinze, W.J., (Ed.), *The Utility of Regional Gravity and Magnetic Anomaly Maps*, Soc. Expl. Geophys., pp: 181-197.

Dames and **Moore** (1988) *Water Resources Development*, *Al-Lith Basin*, Final Report, Vol. **E**., Ministry of Agricultural and Water, Riyadh, Saudi Arabia.

Dames and **Moore** (2001) *Hydrogeological Studies of Wadi Malakan Basin, Water and Sewage Authority of Makkah Al-Mukarramah*, Final Report, Vol. **3**, (in Arabic).

Keating, P. and **Pilkington, M.** (2004) Euler deconvolution of the analytic signal and its application to magnetic interpretation, *Geophysics*, **52**: 165-182.

German Consult (1979) *Investigation and Detailed Studies for the Agricultural Development of South Tihama*, Final Report and Preliminary Design for Ministry of Agricultural and Water, Riyadh, Saudi Arabia.

Hansen, R.O., Pawlowski, R.S. and **Wang, X.** (1987) Joint use of analytic signal and amplitude of horizontal gradient maxima for three-dimensional gravity data interpretation, *57th Ann. Internat. Mtg., Soc. Expl. Geophys.*, Expanded Abstracts, 100-102.

Hartman, R.R., Teskey, D.J. and **Friedberg, J.L.** (1971) A system for rapid digital aeromagnetic interpretation, *Geophysics*, **36:** 891-918.

Jain, S. (1976) An automatic method of direct interpretation of magnetic profiles, *Geophysics,* **41**: 531-541.

Moore, T.A. and **Al-Rehaili, M.H.** (1989) Geologic map of Makkah quadrangle, sheet 21D, Kingdom of Saudi Arabia: DGMR, Geoscience Map **GM-107C**, 1:250,000 scale.

Nabighian, M.N. (1972) The analytic signal of two-dimensional magnetic bodies with polygonal cross-section: Its properties and use for automated anomaly interpretation, *Geophysics*, **37:** 507-517.

Nabighian, M.N. (1974) Additional comments on the analytic signal of two-dimensional magnetic bodies with polygonal cross-section, *Geophysics*, **39:** 85-92.

Nabighian, M.N. (1984) Toward a three-dimensional automatic interpretation of potential field data via generalized Hilbert transform: Fundamental relations, *Geophysics*, **49:** 780-786.

Naudy, H. (1971) Automatic determination of depth on aeromagnetic profiles, *Geophysics*, **36:** 717-722.

Pallister, J.S. (1982c) *Reconnaissance Geologic Map of Harrat Tuffil Quadrangle*, sheet 20/39B, Kingdom of Saudi Arabia, Saudi Arabian Deputy Ministry for Mineral Resources Open-File Report USGS-OF-03-33, scale 1:100,000.

Pallister, J.S. (1986) *Geologic Map of Al-Lith Quadrangle*, sheet 20D, Kingdom of Saudi Arabia: DGMR, Geoscience map **GM-95**, 1:250,000 scale.

Reid, A.B., Allsop, J.M., Granser, H., Millet, A.J. and **Somerton, I.W.** (1990) Magnetic interpretation in the three dimensions using Euler deconvolution, *Geophysics*, **55:** 80-91.

Sogreah (1968) *Water and Agricultural Development Survey for Area IV*, Final Report, Ministry of Agricultural and Water, Riyadh, Saudi Arabia.

Spector, A. and **Grant, F.S.** (1970) Statistical models for interpreting aeromagnetic data, *Geophysics*, **35:** 293-302.

Stavrev, P.Y. (1997) Euler deconvolution using differential similarity transformations of gravity or magnetic anomalies, *Geophys. Prosp*., **45**(2): 207-246.

Stavrev, P., Gerovska D. and **Araúzo-Bravo, M.J.** (2003) Euler deconvolution of magnetic anomalies over the basaltic bodies in northern Bulgaria, *Annual*, vol. **46**, part 2, Geology and Geophysics, Sofia, 2003, pp. 403-407.

Subyani, A.M., Bayumi, T.H., Metsah, M.E. and **Al-Garni, M.A.** (2004) *Quantitative and Qualitative Evaluation of Water Resources in Wadi Malakan and Wadi Adam Basins, Makkah Area*, Final Report 205/422, King Abdulaziz University, Jeddah, Saudi Arabia.

Thompson, D.T. (1982) EULDPH-A new technique for making computer-assisted depth estimates from magnetic data, *Geophysics*, **47:** 31-37.

Torrent, H. and **Sauveplan, C.** (1977) *Orientation Map for Groundwater Exploration Related to Mineral Investigation in the Arabian Shield, Bureau De Recherches Geologiques Et Minires*, Saudi Arabia Mission, BRGM report 77 JED 13, Ministry of Petroleum and Mineral Resources, Jeddah, 6 p.

Vacquier, V., Steenland, N.C., Handerson, R.G. and **Zietz, I.** (1951) Interpretation of aeromagnetic maps, *Mem*., **47:** Geol. Soc. Am.

Zohdy, A.A. (1989) A new method for the automatic interpretation of Schlumberger and Wenner sounding curves: *Geophysics*, **54**: 245-253.

Zohdy, A.A., Bisdorf, R.J. and **Gates, J.S.** (1994) *A Direct Current Resistivity Survey of the Beaver Dam Wash Drainage in Southwest Utah, Southwest Nevada, and Northwest Arizona*, U.S. Geological Survey Open-File Report 76-324, 77 p.

Zohdy, A.A., Eaton, G.P. and **Mabey, D.R.** (1974) Application of surface geophysics to groundwater investigation, *Techniques on Water-Resources Investigations of the United States Geological Survey*, book 2, Chapter D1, 116p.

تطبيق الطرق الجيوفيزيائية المغنطيسية والكهربائية لاستكشاف المياة الجوفية في وادي ملكان ، المملكة العربية السعودية

منصور عبدالله القرني

قسم الجيوفيزياء ، كلية علوم الارض ، جامعة الملك عبدالعزيز

جـــدة – المملكة العربية السعودية

المستخلص . تم استخدام الطرق الكهربائية والمغنطيسية في وادي ملكان ، منطقة مكة المكرمة . الطريقة المغنطيسية طبقت على منطقة الدراسة ليتم التعرف على التراكيب الجيولوجية الأساسية والأعماق لصخور القاعدة . تم استخدام طريقة أويلر الثنائية الأبعاد في تفسيرات البيانات المغنطيسية لإيجاد الأعماق إلى الصخور والتراكيب الجيولوجية التي ربما تؤثر على تدفق المياه الجوفية . استخدمت الطريقة الكهربائية في هذه الدراسة حيث أنه استخدم المسح الأفقي باستخدام توزيع أقطاب فنر والمسح الرأسي باستخدام توزيع أقطاب شلمبيرجير . طريقة فنر استخدمت على طول البروفيلات ليتم التعرف على الأماكن ذات المقاومة النوعية الأقل وإيجاد المكان الأفضل لعمل مسح سبري . ومن ثم تم استخدام المسح السبري باستخدام شلمبيرجير لتحديد النطاقات المشبعة بالماء ، وكذلك تحديد أعماق صخور القاعدة . ولهذا فإن استخدام الطريقة الكهربائية مع الطريقة المغنطيسية أعطى معلومات قيمة عن مناطق تواجد النطاقات المشبعة بالماء المتعلقة بالتراكيب الجيولوجية في منطقة الدراسة . وتم التأكد من التفسيرات الكهربائية بطريقة الحفر عند VES6004 و VES6010 وأظهرت تطابقًا جيدًا . ومن معرفة الأعماق الحقيقية بواسطة الحفر ، تم حساب معامل عدم التجانس coefficient of anisotropy ، ووجد أنه قليل جدًا مما يوضح أن الرواسب الوديانية غير متطبقة .